

Field-Induced Interfacial Properties of Gold Nanoparticles in AC Microelectrophoretic Experiments

Kathryn D. Klopper,[†] Tiberiu-Dan Onuta,[‡] Dragos Amarie,[‡] and Bogdan Dragnea^{*,†,‡}

Department of Chemistry, Indiana University, Bloomington, Indiana 47405-7102, and
Department of Physics, Indiana University, Bloomington, Indiana 47405-7105

Received: June 10, 2003; In Final Form: November 5, 2003

Electrophoretically induced aggregation of Au nanoparticles has been studied in the past especially in relation to interparticle interactions or particle/surface interactions leading to self-organization of particles into structures. The work described here focuses on field-induced interfacial changes preceding the aggregation. We show that, in strong AC electric fields, comparable to those used for electrophoretic aggregation of microwires and 2D crystals at electrode surfaces, slow field-dependent variations in the nanoparticle mobility occur. These variations in mobility are accompanied by a few orders of magnitude increase in the adsorption rate of colloidal gold nanoparticles, onto a similarly charged silica surface. The onset time of adsorption strongly depends on the applied AC field intensity. A qualitative model aimed at explaining the observed field-induced adsorption of negatively charged gold particles on a similarly charged silica surface is proposed. The model is based on the idea that the adsorbed ion distribution at the particle surface is influenced by the applied electric field. The result of prolonged electric field exposure is a nonuniform distribution of charge across the nanoparticle surface, which renders orientation-dependent adsorption possible.

Introduction

One of the most prominent features of the separation region between two phases is the rearrangement with respect to bulk of ions, electrons, and dipolar constituents to minimize their interfacial free energy.¹ In the case of an interface between a solid and an electrolyte solution, the rearrangement of charges takes the form of an electrical double layer composed of the surface charge on the particle and a distribution of counterions in solution. Due to its pivotal importance in electrochemistry, biomembrane processes, and rheology of complex fluids, the structure of the double layer has been extensively studied for the past 200 years.^{2,3} However, because of the complexity of the systems involved, new phenomena and challenges pertaining to the electrical double layer continue to be unveiled.^{4,5} For example, the strong interest in the possibility of generating new hierarchical materials by electrophoretically induced aggregation of colloidal particles⁶ led to two remarkable findings. One is the formation of electrically functional microwires from gold nanoparticle suspensions.⁷ The other is the field-controlled assembly of colloidal particles into extended 2D and 3D crystals on the surface of an electrode.^{6,8,9}

An intriguing characteristic of these field-induced processes is that quite similar conditions (particle size, material, field amplitude, and frequency) seem to lead to very different structures requiring different dominant mechanisms of organization. For instance, the microwire growth in aqueous suspensions of gold nanoparticles in AC fields requires the existence of a sharp tip formed from an elongated cluster of nanoparticles to generate intense field gradients.⁷ The sharp tip can form only if initial multilayer growth takes place. However, this is in opposition to the demonstrated monolayer growth in both AC

or DC electrophoretic deposition and gold colloid lattice formation.^{8,10}

Detailed studies aiming to reveal the parameters influencing the aggregate morphology showed that, besides direct electrophoretic pressure,¹¹ electrohydrodynamic flows generated by reactions at the electrode surface have an important role in particle–particle and aggregate–aggregate interactions.^{12–14} The aggregate growth close to the electrode surface is consequently the result of a delicate balance between electrostatic and electrohydrodynamic factors.

Most of the work dedicated to field-induced aggregation focused directly on the growth process, i.e., at instances where the particle is already close enough to the surface to experience interactions leading to irreversible association. The goal of this paper is to show that, when strong fields and conductive particles are employed, field-induced changes in the interfacial properties of the particles occur even before this interaction stage. Such variations in the interfacial properties of gold colloidal particles may subsequently influence adsorption kinetics.

The electrophoretic mobility of single gold particles, 200 nm in diameter, was monitored by dark-field video microscopy during AC electrophoresis experiments. Both standard deviation of the mobility distribution and the average mobility exhibit changes proportional to the applied field. After a certain amount of field exposure, the negatively charged particles in electrophoretic oscillation between the electrodes adsorb on the similarly charged fused silica window. Particles, which are dispersed in the same solution, but outside the field lines, do not adsorb. A qualitative model, outlined in the Discussion section, based on nonuniform surface charge redistribution provides a tentative explanation of the observed correlation between particle adsorption and mobility changes.

Experimental Section

Electrophoretically driven oscillatory motion of individual gold particles 200 nm in diameter (purchased from Ted Pella,

* Address correspondence to this author. E-mail: dragnea@indiana.edu.

[†] Department of Chemistry.

[‡] Department of Physics.

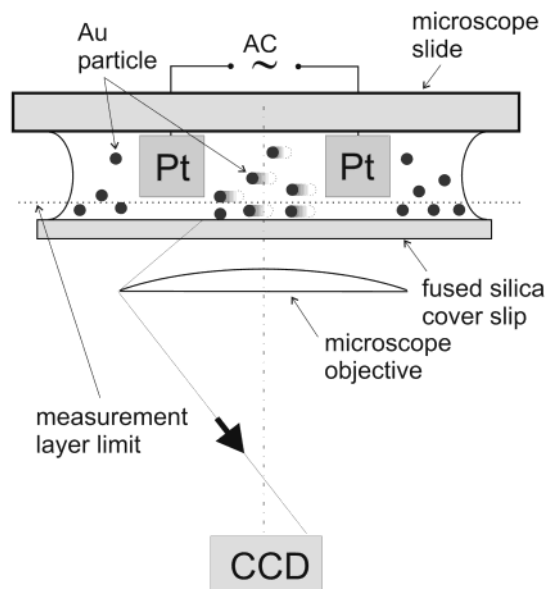


Figure 1. Schematic of the AC electrophoretic experiment. Focused white light (400–600 nm) from above is scattered by the gold particles, collected by the microscope objective, which focuses on the bottom of the cell, and projected onto the CCD camera. The amplitude of oscillation of individual Au particles 200 nm in diameter is measured from the time-averaged trace with use of CCD integration times longer than the oscillation period, but short enough to prevent significant lateral diffusion during the measuring time window. The dotted line represents the limit of the optical depth of field.

Inc., size dispersion less than 20%) has been monitored by video microscopy with a dark-field microscope¹⁵ (Nikon TE300, microscope objective: 60 \times , numerical aperture (NA) = 0.75) equipped with a CCD camera (EDC-2000, Electrim). The gold particles were suspended at a number concentration of 1.8×10^8 particles/mL in an aqueous solution of trisodium citrate, at pH 8.0. The slightly basic pH ensures that the adsorbed citrate groups on the gold particle surface should be almost completely dissociated. To confirm this hypothesis and identify other possibly adsorbed groups we have used micro-Surface Enhanced Raman Spectroscopy (SERS) on surface-immobilized selected particles in solution. The ionic strength of the buffer solution was 10^{-4} M, corresponding to a Debye screening length of ~ 30 nm. High-purity, MilliQ-grade water was used for all buffer solutions and cell surface conditioning. Glass parts were stored in water after initial cleaning in *aqua regia* to achieve a stationary state of the surface.¹⁶ Prior to each experiment, all parts of the cell were carefully cleaned first by an alkaline cleaning solution, then rinsed with water, methanol, and again water. The electrophoretic cell, Figure 1, is built from a borosilicate glass microscope slide stacked together with a fused silica cover slip. In the presence of aqueous solution, the liquid-filled gap between the cover slip and the microscope slide is maintained by capillary forces at $\sim 80 \mu\text{m}$. The distance between the two microelectrodes made of 70 μm thick Pt foil is 1.0 mm. A function generator delivered the AC sinusoidal bias (0–10 V peak-to-peak, 0–100 Hz). The microscope is focused on the upper surface of the cover slip, which is immersed in solution. Filtered white light (450–580 nm) is incident from a dark-field condenser on the particles at angles corresponding to 0.80–0.95 NA. Since the theoretical depth of field is ~ 500 nm and the objective focuses on the bottom of the cell (Figure 1), only those particles having their centers in a layer between ~ 100 nm (corresponding to surface contact) and ~ 500 nm above the surface are measured. The camera exposure time is set to be equal to one period of the AC bias, typically, 10–100 ms.

The maximum current through the cell is less than $10 \mu\text{A}$. In these conditions, electrolytic reactions at the electrodes resulting in electrode polarization or heating with subsequent formation of gas bubbles and thermal convection are negligible.¹⁷

Results

The Origins of the Surface Charge. The initial charge on the particles has been estimated by DC gel electrophoresis.¹⁸ We found that the gold particles are negatively charged in solution with a net charge of 60×10^{-18} C.

The measured SERS vibrational spectrum of surface-immobilized Au particles is dominated by the presence of bands near 1400 cm^{-1} , corresponding to vibrations of the COO^- group, probably due to adsorbed citrate ions. The absence of the characteristic “carbonyl” frequency band at 1700 cm^{-1} , from all the spectra of gold particles in solution with basic pH, has been noticed. This is indicative of complete ionization of the citrate groups.¹⁹

Other possible groups identifiable in the SERS spectra are AuOH^- (stretching, 577 cm^{-1})²⁰ and AuCl^- (several frequencies in the 350-cm^{-1} region).²¹ The adsorbed Cl^- ion is probably coming from the initial HAuCl_4 reactant used at the preparation of gold particles. The SERS analysis points therefore to a net charge at the surface that results from specific adsorption of several ionic species.

Lateral Diffusion in the Absence of an Electric Field. In the absence of an external field, after a few minutes from the introduction of the sample, the gold particles sediment and settle in a layer above the bottom surface of the cell. Due to the negative charge of the silanol groups on the fused silica surface,²² of approximately $-10 \mu\text{C}/\text{cm}^2$, the negatively charged gold particles “hover” above the surface in slow lateral Brownian motion, remaining most of the time within the depth of field of the microscope objective.

Measuring the lateral Brownian diffusion of particles is useful to assessing whether the properties of the fluid layer where the particles settle vertically are different from the properties of bulk fluid. A possible origin for such deviations from the bulk properties would be the presence of a patch-charged surface, which, in turn, could play a role in the particle adsorption.

If the silica surface charge is heterogeneous at a scale of ~ 100 nm, the resulting double layer interaction potential between the surface and the particle should have local variations. The particle would have to hop across local potential barriers. The lateral diffusion coefficient would then be lower than the one for bulk diffusion.

The calculated gravitational settling time³ corresponding to half of the cell height, for 200-nm diameter gold particles in water at 25 $^\circ\text{C}$, is 130 s. This is significantly smaller than the time required to cover the same distance in Brownian motion:³ ~ 600 s. Therefore, the dominant forces in the vertical direction (normal to the cell surface) are the electrostatic force between the particle and the surface and the gravitational force. Knowing that the layer in which the particles settle is within the optical measurement range of 100 to 500 nm above the surface, one can estimate the maximum limit for the surface charge, which stabilizes the particle against the gravitational force.

The equilibrium condition is

$$F_e = F_g - F_b \quad (1)$$

where F_e is the electrostatic force, F_g is the gravitational force, and F_b is the buoyancy force.

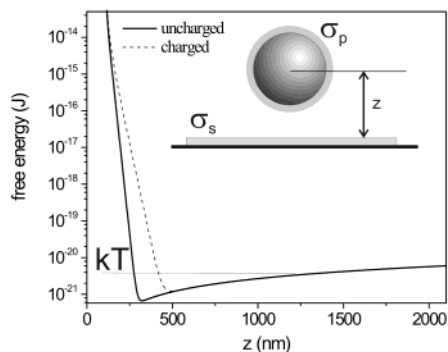


Figure 2. Calculated total (electrostatic and gravitational) energy dependence on the distance between the center of a colloidal particle, 200 nm in diameter, and a negatively charged glass surface (dashed line, $2.0 \mu\text{C}/\text{cm}^2$; continuous line, $0 \text{ C}/\text{cm}^2$). The particles can move laterally in Brownian diffusion, but are constrained to a certain layer ($\sim 700 \text{ nm}$ thick) in the direction normal to the surface.

For small surface charge densities, the free energy of interaction per unit area between two flat surfaces is approximated by²³

$$W_{\text{dl}}(z) \approx \frac{1}{\kappa \epsilon_0 \epsilon_r} \left[\frac{(\sigma_p^2 + \sigma_s^2) e^{-\kappa(z-a)} + 2\sigma_p \sigma_s}{e^{\kappa(z-a)} - e^{-\kappa(z-a)}} \right] \quad (2)$$

where z is the position of the particle center above the surface, κ^{-1} is the Debye length (30 nm), σ_p is the unknown surface charge density of the gold particle, σ_s is the surface density of the silica ($-11 \mu\text{C}/\text{cm}^2$), ϵ_0 is the vacuum permittivity ($8.85 \times 10^{-12} \text{ J}^{-1} \text{ C}^2 \text{ m}^{-1}$), ϵ_r is the relative permittivity of water (80), and a is the particle radius. The rather crude approximation of the interaction between the sphere and the surface, using the two flat surfaces model justified for large sphere radii, is used here only with the purpose of evaluating the order of magnitude of the surface charge involved and illustrating the principles of the experiment.

The gravitational energy of a particle at the distance z from the surface is

$$E_g(z) = (\rho_s - \rho_l) \frac{4\pi a^3}{3} g z \quad (3)$$

The averaged gravitational energy per unit area of the sphere is

$$W_g(z) \approx \frac{4}{3} (\rho_s - \rho_l) a g z \quad (4)$$

The equilibrium condition (1) provides then an equation from which σ_p can be estimated when the equilibrium position z_0 above the surface is known:

$$\frac{\partial W}{\partial z} = \frac{\partial}{\partial z} \left[\frac{2\kappa^{-1} \sigma_p \sigma_s}{\epsilon_0 \epsilon_r} e^{-\kappa z} - \frac{4}{3} (\rho_s - \rho_l) a g z \right]_{z=z_0} = 0 \quad (5)$$

The total free energy due to gravitational and electrostatic forces has been represented in Figure 2 as a function of the distance between the particle center and the surface, z . From this calculation, the surface charge density has to be less than $2.0 \mu\text{C}/\text{cm}^2$, which corresponds to a shallow minimum in the total potential energy, W , located at the limit of the optical depth of field (500 nm above the surface). Due to the existence of the minimum in $W(z)$, particles in Brownian motion will be free to move laterally, but constrained vertically to a layer of

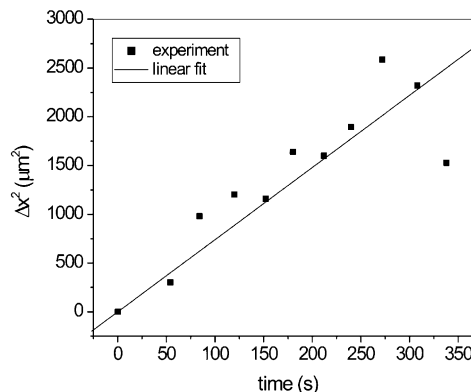


Figure 3. Square displacement of a particle as a function of time and linear fit used to find the lateral diffusion coefficient.

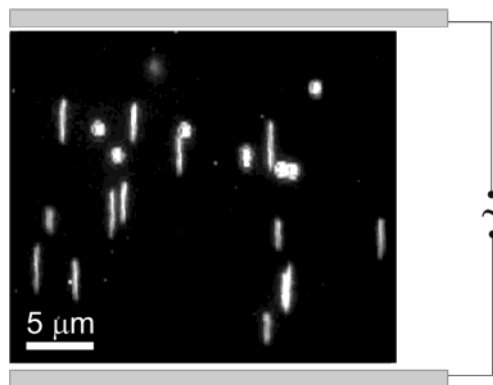


Figure 4. Electrophoretic dithering of 200 nm gold nanoparticles. Electric field intensity: 10 kV/m. Frequency: 15 Hz. CCD exposure time: 70 ms. The circular bright spots are adsorbed particles on the bottom surface of the cell. Note the large variations of the averaged trajectories between particles.

thickness comparable to the depth of field of the microscope, conveniently offering the possibility of optical tracking.

The diffusion coefficient has been evaluated from plots of the root-mean-square lateral displacement vs time, using the Einstein–Smoluchowski equation³

$$\langle \Delta x^2 \rangle = 2Dt \quad (6)$$

For a 200-nm diameter gold particle in water at 25 °C, the calculated diffusion coefficient is $2.5 \times 10^{-12} \text{ m}^2/\text{s}$. The experimental diffusion coefficient, estimated by using (6) to fit the experimental data, is $3.2 \times 10^{-12} \text{ m}^2/\text{s}$, Figure 3. The slight difference between the experimental and calculated diffusion coefficients may be due to heating of the sample by the microscope lamp or to the presence of small convection currents. Since there is no noticeable slowing down of the Brownian motion close to the surface, we infer that, even if patch charging may occur, the electrostatic potential is smooth over the spatial range probed by the particle ($\sim 100 \text{ nm}$).

Gold Particles under the Influence of an Applied AC Field. When an AC field is applied, the gold particles start oscillating. Typical time-averaged trajectories during an oscillation period are presented in Figure 4.

Acquiring successive frames to follow individual particles reveals an interesting characteristic: the amplitude of oscillation shows temporal fluctuations that are too broad to be explained as thermal agitation effects, Figure 5. Calculations of the Brownian displacement over the integration time window of the CCD camera show that thermal fluctuations in the amplitude of oscillation should be of the order of 300 nm. However, on

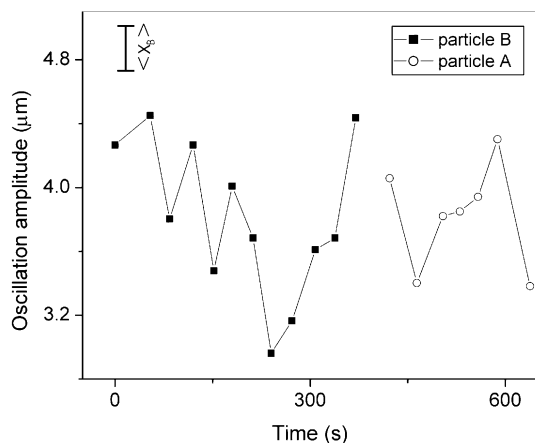


Figure 5. When tracking individual particles across a series of video frames, large fluctuations in the amplitude of oscillation under an AC field can be noticed. The fluctuations exceed several times those accounted for by the Brownian fluctuation theory applied to the integration time window ($\langle x_B \rangle = 300$ nm).

Figure 5 one can notice variations of the order of $1 \mu\text{m}$, which persist on times scales of 100 s.

These large-scale fluctuations could be due to the particle drifting vertically in Brownian motion inside the potential well of Figure 2. The diffuse charge concentration varies rapidly with the vertical coordinate (ca. $\exp(-\kappa z)$). Electrokinetic properties of the dithering particle will then depend on the vertical particle coordinate within the optical depth of field. Another possible origin is actual surface charge fluctuations in time. The amount of the surface charge depends on the surrounding ionic cloud. For small numbers of charges on the surface and low ionic strengths, statistical fluctuations may become important. To the best of our knowledge, the temporal diffusion of the surface charge has not been addressed yet, most electrokinetic studies concentrating on the average properties of ensembles of particles. However, to unambiguously determine the cause of these slow fluctuations a combination of at least two methods is needed: for instance, a high spatial resolution interferometric method to determine the position normal to the surface, simultaneously employed with a method like the one presented here to determine the particle mobility.

Finding the relationship between the velocity of the particle per unit field intensity and the electrical double-layer characteristics has been the subject of study for many years.^{2,3} Our goal is to determine whether there is a direct influence of the applied electrical field on the surface properties of gold particles, which might influence the way particles interact between them or with surfaces. To this end, we follow individual particles exposed to intense AC fields by measuring their individual mobilities. In general, the applied field induces both liquid displacement with respect to the silica surface (electroosmosis) and motion of suspended particles with respect to the fluid (electrophoresis). However, it has been shown, in electrophoretic experiments inside capillaries, that a particle reaches a stationary velocity much faster than the liquid.²⁴ Thus, using AC fields and relatively high frequencies reduces the effect of electroosmotic effects. In our experimental configuration, the fluid is confined to the space between the microscope slide and the cover glass, and therefore a similar behavior as in capillaries is expected. Moreover, even if some electroosmotic effects persist, the fact that we measure at a constant height above the silica surface still makes possible detecting relative mobility variations indicative of changes of electrical surface properties of particles.

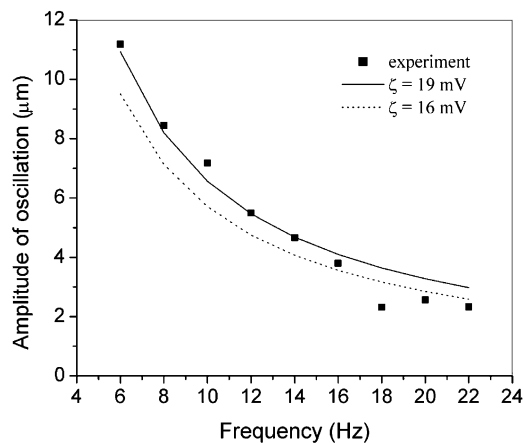


Figure 6. Amplitude of oscillation vs frequency of the applied field. Squares: experimental data. Continuous line: least-squares fit with (9) for all data points. Dotted line: least-squares fit with (9) for data points above 12 Hz, with the ζ -potential as the fit parameter. Field intensity: 5 kV/m.

The particles follow the alternating electric field according to their DC mobility for oscillation periods well below the time necessary for ion density changes to spread out into the electrolyte ($\sim 10^{-5}$ s). For spherical particles, the relationship between the particle velocity and the intensity of the applied field is³

$$v = \mu_E E \quad (7)$$

where μ_E is the electrophoretic mobility of the particle.

For thin double layers, the Smoluchowski formula relates mobility to the ζ -potential and the fluid viscosity:

$$v = \frac{\epsilon \zeta E}{\eta} \quad (8)$$

One can integrate (8), for a sinusoidal time-dependent bias, to obtain the particle trajectory as a function of time:

$$x(t) = \frac{\epsilon \zeta U}{\omega \eta d} \cos(2\pi \nu t - \phi) \quad (9)$$

where U is the maximum voltage and d is the distance between electrodes (1 mm). The mobility can be thus estimated from the amplitude of oscillation, which we measure directly from data like those shown in Figure 4. Measuring the amplitude of oscillation as a function of frequency yields the dependence represented in Figure 6. The experimental data can be fitted by a hyperbolic dependency of ω as predicted by (9). If electroosmotic effects were present, the low-frequency data should have a different fit parameter than the high-frequency data.²⁴ Separate fitting of the high-frequency data does not yield very different results, Figure 6. We deduce that, in our case, the presence of electroosmotic effects is not significant. When we use (9) to estimate the electrophoretic mobility, we find $\mu_E = 0.012 \mu\text{V}/\text{m}^2/\text{s}$.

From the Smoluchowski formula for electrophoretic mobility applied to data in Figure 6, the ζ -potential is 19 mV, which is of the same order of magnitude with the reported ζ -potential of 35 mV for 20-nm diameter citrate-stabilized colloidal gold particles.²⁵ The total surface charge can be approximately evaluated from mobility with³

$$Q_E \approx 6\pi\mu_E\eta a \quad (10)$$

yielding the numerical result $Q_E = 22 \times 10^{-18}$ C, in satisfactory

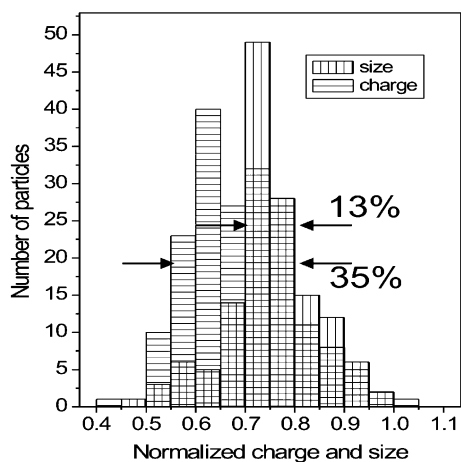


Figure 7. Normalized charge and size distributions. The full width at half-maximum of the histograms is indicated as a percentage of the average values. The charge distribution is broader and more asymmetric with respect to the size distribution.

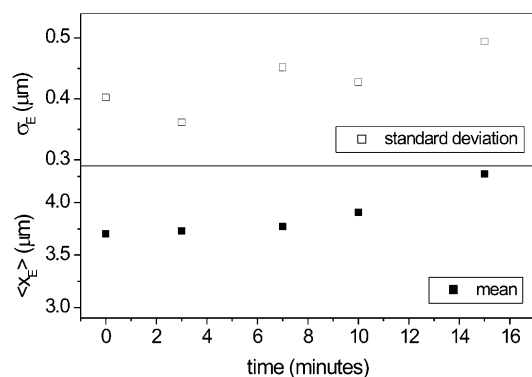


Figure 8. Mean oscillation amplitude (solid squares) and standard deviation (open squares) vs time. Field intensity: 5 kV/m. Frequency: 15 Hz.

agreement with the independent determinations by DC gel electrophoresis.

The method of electrophoretic oscillation outlined here is straightforward to use for determinations of surface charge distribution among an ensemble of particles. As is shown in Figure 7, the surface charge has a significantly different distribution than the particle size. This aspect, directly demonstrated here for the first time, has a particular importance for material sciences areas focusing on composite materials with nanoparticles as building blocks. The results in Figure 7 suggest that even for a size-monodisperse sample, there will be a spread in surface properties. This is an important point for material science areas focusing on composites, and using nanoparticles as building blocks.²⁶ It shows that both size and surface chemistry control have to be achieved to obtain homogeneous materials with reproducible properties.²⁷

The two normalized distributions in Figure 7 should overlap, if a uniform surface charge density, independent of the particle radius, described the surface charge distribution at the solid/liquid interface. The histograms in Figure 7 indicate, however, that this is not the case. Furthermore, during the AC field exposure, both spread of the charge distribution and average mobility values are found to increase, Figure 8.

After these changes in the amplitude of oscillation, increased adsorption of exposed particles to the AC field takes place on the silica surface between the electrodes. The number of adsorbed particles is plotted vs time in Figure 9, with the electric field intensity as the parameter.

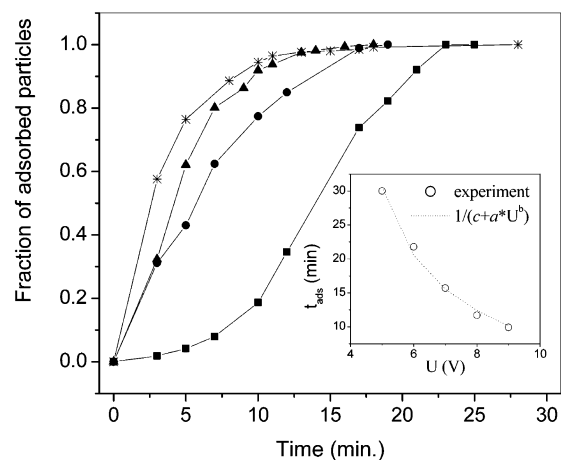


Figure 9. Fraction of adsorbed particles vs time with electric field intensity as the parameter: (squares) 4 kV/m; (circles) 4.7 kV/m; (triangles) 5.3 kV/m; and (stars) 6 kV/m. Fixed frequency: 15 Hz. Inset: adsorption time (defined as the time that it takes for 95% of the present particles to be adsorbed) vs applied bias (dots) and fit according to a model based on the possible role of the fluid washing the particle surface.

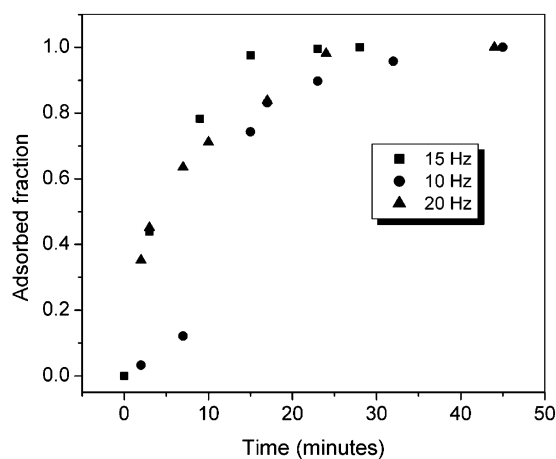


Figure 10. Fraction of adsorbed particles vs time with frequency as the parameter.

To see if it is changes in the cell silica surface or the particle surface that lead to adsorption, we have preserved the same silica surface from previous experiments, but introduced fresh (unexposed) particles. The unexposed particles did not exhibit increased adsorption on preexposed silica surfaces. Adsorption kinetics followed the same dependence on field as fresh particles on cleaned surfaces (Figure 9).

A slight increase ($\sim 2\%$ over 20 min.) in the cell conductance is noticed during the experiment. However, salt addition to increase by the same amount the ionic strength of solution does not lead to noticeable enhanced adsorption or increase in particle mobility.

While the field intensity has a strong influence on the adsorption process, the frequency seems to play a less important role, at least below 20 Hz, Figure 10.

Discussion

The increase in oscillation amplitude with time observed during our experiments could have two origins: (a) a variation in the ionic strength of the solution due to impurities participating in electrochemical processes and (b) a variation in the electric surface properties of the gold particles. However, the 2% increase in the cell conductance points to an increase in the

ionic strength, which would rather lead to a drop in mobility according to the Henry theory.³ Thus, we deduce that a change in the surface properties is at the origin of the oscillation amplitude increase.

From Figure 8, mobility maintains the same sign, but increases over time. How is it then possible that an increase in the negative surface charge would result in stronger adsorption on negatively charged silica? We have seen that the silica surface is not responsible for the adsorption enhancement: fresh particles do not adsorb on already exposed surfaces. Also, particles immersed in the same solvent, but placed in regions with negligible electric fields, do not adsorb. We infer from these facts that changes in the surface charge properties occur during the electrophoretic dithering and these changes are related to the enhanced adsorption in the space between electrodes. As seen in Figures 8 and 9, changes are proportional to the field intensity and less sensitive to frequency.

The only remaining explanation for the adsorption of negative particles on a negative surface is a nonuniform distribution of ions on the particle surface reached as a result of exposure to the electric field. It is known that particles that are patch-charged are more prone to adsorption or aggregation.²⁸ The question is: By what mechanism does the field change the surface charge distribution? At this time, we can only provide a qualitative explanation.

In the case of conducting particles undergoing electrophoresis, currents may pass through the particle surface. This is in stark contrast with respect to the much better studied dielectric particles²⁹ for which the electrolyte streamlines are not strongly distorted by the particle.² Intersection of the particle surface by streamlines is known to generate over voltages and polarization effects in the double layer.³ The interfacial charge depends on interactions of surface groups with ionic species in solution.³⁰ Any variation of the local ionic environment will thus lead to a local fluctuation in the surface charge.³¹ In sufficiently intense fields, like those close to the surface of a metallic particle, there is deformation of the electrical double layer, which means that the ion concentration in the electrical double layer will depend on the local field polarization. For a sphere in a fixed position with respect to the field direction, all electrical layers (diffuse, stagnant, chemisorbed ions) are expected to be influenced by the field, with different relaxation times.^{30,32} If left enough time, the entire electrostatic system (not only the diffuse layer) will adapt to reflect the field presence, which means that induced anisotropy of the surface charge is expected, as well. At first sight, rapid rotational diffusion during the AC electrophoresis would effectively average the orientation of the particle in the field. Nevertheless, this is true only when the adsorbed ions are uniformly spread over the particle surface. If, due to the discreteness of charge^{33,34} or islandlike charge organization,³⁵ an initial dipole moment exists, the particle orientation in the field will not be random anymore.

We show in the following that a reasonably small initial dipole moment would be enough to maintain the same particle orientation with respect to the electrophoretic field. This means that the particle hemisphere that always faces the anode is likely to harbor a different electrochemistry than the other hemisphere, hence the development of anisotropy.

The energy of a dipole in a uniform field is³⁶

$$W_{\text{dipole}} = pE \cos(\theta) \quad (11)$$

where p is the dipole moment, E is the field intensity, and θ is the angle between the dipole axis and the field. The energy of a dipole created by an unbalance of only one elementary charge

across the diameter of the particle is of the order of 3×10^{-22} J, which is just 1 order of magnitude less than kT . It follows that for spheres, which would initially have a charge unbalance equivalent to 10 electrons between two opposite hemispheres, the AC field induced orientation overcomes the rotational diffusion. Therefore, the particles are likely indeed to be oriented with the same hemisphere toward the electrode of opposite polarity. Constant orientation with respect to the field might lead, as we have seen, to a supplemental field-induced anisotropy of the surface charge, which, in turn, results in different electrokinetic behavior and finally the possibility of adsorption.

The fact that the particles are in constant motion raises the question whether the liquid flow washing the particle surface does not speed a process that would occur in fact even without the electric field, but at longer times (like a surface reaction due to contaminants). In such a model, the adsorption time (defined as the time required to adsorb the majority of the particles) is proportional with the volume of fluid effectively "seen" by the particle due to its motion. This electrolyte volume is linearly proportional to the applied bias and does not depend on frequency (from eq 8). Using this model we have obtained a general fitting function of the form

$$t_{\text{ads}}(U) = \frac{1}{c + aU^b} \quad (12)$$

where $1/c$ represents the time it would take for the surface reaction to occur in the absence of the field, a represents a proportionality constant depending on viscosity and particle diameter, and b is an exponent coming from the order of reaction. From the fitting in Figure 9, $1/c = 125$ min and $b = 2.5$. If this model is correct, adsorption of $\sim 95\%$ of particles should occur after approximately 2 h in the absence of the electric field. This is not what we observe; negligible absorption occurs even for times longer than ~ 10 h.

To adsorb onto silica, the particles have to achieve orientations corresponding to a minimum of the dipole energy in the surface electrical field. In this case, closer distances between surfaces are possible and van der Waals forces may exceed the repulsive Coulomb forces leading to irreversible adsorption. What dipole momentum should the particle achieve to overcome the Coulomb repulsion due to the net surface charge? In a first, coarse approximation, the total energy of a particle inside the double layer of the silica surface can be estimated from the energy of the net charge on the particle plus the energy of the dipole in the nonuniform electric field of the surface:

$$W(z) = W_{\text{el}}(z) + p \frac{d\Phi}{dz} \quad (13)$$

where $W_{\text{el}}(z)$ is given by eq 2, and $d\Phi/dz \approx 10^6$ V/m. For the particle to reach within 2 nm from the silica surface (the van der Waals range) the dipolar momentum p should be of the order of 10^{-21} C·m, which accounts for ca. 10^4 elementary charges separated across the particle diameter.

The characteristic of orientation-dependent adsorption is reminiscent of problems encountered in random sequential adsorption^{37–40} where one attempts to irreversibly place objects on a surface in a way that satisfies certain lateral constraints. Using a model inspired from random sequential adsorption, it thus should be possible to link the rate of adsorption and the charge anisotropy. However, the actual spatial distribution, which we ignore at the moment, has to be known to calculate the rate of adsorption. Due to the fact that dramatic qualitative differences in electrokinetic properties may occur for different

surface charge patterns, an independent method of direct determination of surface charge distribution would be required to attempt the numerical simulation of data in Figure 8.⁴¹ To this end, second harmonic generation experiments are on their way in our laboratory. If successful, these experiments will provide a direct estimate for surface charge anisotropy and an additional workbench for further use of such models.

Conclusion

The AC electrophoretic trajectories of individual citrate-stabilized gold particles have been followed in time to reveal changes in the electrokinetic parameters. Such changes are proportional to the exposure to the electric field. We have shown that 200-nm gold particles have a surface charge distribution that is qualitatively different from the size distribution, which implies that the model of a surface charge density independent of size does not apply in this case. The average surface charge and the breadth of the surface charge distribution increase during exposure to AC electric fields greater than 1 kV/m, probably due to redistribution of the charge in all layers of the electrostatic system attached to the particle. Our findings have direct implications for electrophoretic aggregation of particles suggesting that prior to aggregation, the electric field may induce surface charge anisotropy, which will influence the association rate.

Acknowledgment. K.D.K. is grateful for a NSF-REU summer scholarship. Partial support for this project comes from NSF grant BES0322767. We are grateful to Dr. J. Zaleski for making available his micro-SERS instrumentation for in situ particle characterization.

References and Notes

- (1) Somorjai, G. A. *Introduction to surface chemistry and catalysis*, 2nd ed.; John Wiley & Sons: New York, 1994.
- (2) Lyklema, J. *Fundamentals of interfacial and colloid science*, 1st ed.; Academic Press: New York, 1995; Vol. 2.
- (3) Hunter, R. J. *Foundations of Colloid Science*, 2nd ed.; Oxford University Press: Oxford, UK, 2001.
- (4) Attard, P. *Curr. Opin. Colloid Interface Sci.* **2001**, *6*, 366.
- (5) Tohver, V.; Smay, J. E.; Braem, A.; Braun, P. V.; Lewis, J. A. *Proc. Natl. Acad. Sci. U.S.A.* **2001**, *98*, 8950.
- (6) Sastry, M.; Rao, M.; Ganesh, K. N. *Acc. Chem. Res.* **2002**, *35*, 847.
- (7) Hermanson, K. D.; Lumsdon, S. O.; Williams, J. P.; Kaler, E. W.; Velev, O. D. *Science* **2001**, *294*, 1082.

- (8) Trau, M.; Saville, D. A.; Aksay, I. A. *Science* **1996**, *272*, 706.
- (9) Rogach, A. L.; Kotov, N. A.; Koktysh, D. S.; Ostrander, J. W.; Ragoisha, G. A. *Chem. Mater.* **2000**, *12*, 2721.
- (10) Giersig, M.; Mulvaney, P. *J. Phys. Chem.* **1993**, *97*, 6334.
- (11) Hamaker, H. C. *Trans. Faraday Soc.* **1940**, *36*, 180.
- (12) Trau, M.; Saville, D. A.; Aksay, I. A. *Langmuir* **1997**, *13*, 6375.
- (13) Rhodes, P. H.; Snyder, R. S.; Roberts, G. O. *J. Colloid Interface Sci.* **1989**, *129*, 78.
- (14) Trau, M.; Sankaran, S.; Saville, D. A.; Aksay, I. A. *Nature* **1995**, *374*, 437.
- (15) Abdel-Fattah, A. I.; El-Genk, M. S.; Reimus, P. W. *J. Colloid Interface Sci.* **2002**, *246*, 410.
- (16) Luthi, Y.; Ricka, J.; Borkovec, M. *J. Colloid Interface Sci.* **1998**, *206*, 314.
- (17) Burns, N. L. Measurement of Electrokinetic Phenomena in Surface Chemistry. In *Handbook of Applied Surface and Colloid Chemistry*; Holmberg, K., Ed.; John Wiley & Sons, Ltd.: New York, 2001; Vol. 2, p 371.
- (18) Rodbard, D.; Chrambasch, A. *Anal. Biochem.* **1971**, *40*, 95.
- (19) Edsall, J. T. *J. Phys. Chem.* **1937**, *5*, 508.
- (20) Murphy, P. J.; LaGrange, M. S. *Geochim. Cosmochim. Acta* **1998**, *62*, 3515.
- (21) Hendra, P. J. *Spectrochim. Acta* **1967**, *23 A*, 2871.
- (22) Bolt, G. H. *J. Phys. Chem.* **1957**, *61*, 1166.
- (23) Parsegian, V. A.; Gingell, D. *Biophys. J.* **1972**, *12*, 1192.
- (24) Minor, M.; vanderLinde, A. J.; vanLeeuwen, H. P.; Lyklema, J. *J. Colloid Interface Sci.* **1997**, *189*, 370.
- (25) Schmitt, J.; Machtle, P.; Eck, D.; Mohwald, H.; Helm, C. A. *Langmuir* **1999**, *15*, 3256.
- (26) Heath, J. R. *Acc. Chem. Res.* **1999**, *32*, 388.
- (27) Alivisatos, A. P.; Barbara, P. F.; Castleman, A. W.; Chang, J.; Dixon, D. A.; Klein, M. L.; McLendon, G. L.; Miller, J. S.; Ratner, M. A.; Rossky, P. J.; Stupp, S. I.; Thompson, M. E. *Adv. Mater.* **1998**, *10*, 1297.
- (28) Bouyer, F.; Robben, A.; Yu, W. L.; Borkovec, M. *Langmuir* **2001**, *17*, 5225.
- (29) Fagan, J. A.; Sides, P. J.; Prieve, D. C. *Langmuir* **2003**, *19*, 6627.
- (30) *Interfacial Dynamics*; Kallay, N., Ed.; Dekker: New York, 1999.
- (31) Hansen, J.-P.; Lowen, H. *Annu. Rev. Phys. Chem.* **2000**, *51*, 209.
- (32) Lyklema, J. *J. Phys.: Condens. Matter* **2001**, *13*, 5027.
- (33) Lukatsky, D. B.; Safran, S. A.; Lau, A. W. C.; Pincus, P. *Europhys. Lett.* **2002**, *58*, 785.
- (34) Kostoglou, M.; Karabelas, A. J. *J. Colloid Interface Sci.* **1992**, *151*, 534.
- (35) Zhmud, B. V.; House, W. A. *J. Colloid Interface Sci.* **1997**, *187*, 509.
- (36) Jackson, J. D. *Classical Electrodynamics*, 2nd ed.; John Wiley and Sons: New York, 1975.
- (37) Senger, B.; Schaaf, P.; Bafaluy, F. J.; Cuisinier, F. J. G.; Talbot, J.; Voegel, J. C. *Proc. Natl. Acad. Sci. U.S.A.* **1994**, *91*, 3004.
- (38) Jin, X. Z.; Wang, N. H. L.; Tarjus, G.; Talbot, J. *J. Phys. Chem.* **1993**, *97*, 4256.
- (39) Viot, P.; Tarjus, G.; Ricci, S. M.; Talbot, J. *J. Chem. Phys.* **1992**, *97*, 5212.
- (40) Ricci, S. M.; Talbot, J.; Tarjus, G.; Viot, P. *J. Chem. Phys.* **1992**, *97*, 5219.
- (41) Long, D.; Ajdari, A. *Phys. Rev. Lett.* **1998**, *81*, 1529.